Supporting Information

To accompany the manuscript entitled

Pathways of Superoxide (O_2^-) decay in the Tropical Atlantic

Kathrin Wuttig, Maija I. Heller and Peter L. Croot

Comprising:

26 Pages

6 Tables

4 Figures

Supplementary Information:

Sampling Stations: The location of the sampling GoFlo-Stations in the Eastern Tropical North Atlantic (ETNA) used in this study can be found in Table S1 and Figure S1. Samples were collected during the Meteor cruise M83/1 (Las Palmas, Gran Canaria, Spain – Mindelo, Cape Verde), from 14 October - 13 November 2010 on board the German research vessel RV Meteor. The cruise was designated as a tracer survey and 6 GoFlo-Stations with two-three casts with 4 GoFlo-bottles each were performed. The first station was located at the Cape Verde Ocean Observatory (former TENATSO, now CVOO) time-series station close to the Cap Verde Island Sao Vicente (17.6°N 24.3°W) (cvoo.geomar.de). The next two stations (2 & 3) were occupied on the Mauritanian shelf and 3 stations in the open ocean (4 – 6). The total trace metal concentrations for all stations are shown in Table S3 and the data of specific metal decay rates of O_2^- in Table S4.

Water Sampling: All analytical work at sea was performed in an over-pressurized ISO class 5 clean container, inside of which analysts wore the appropriate clean room apparel, overalls with hood (Tyvek), shoes (Abeba) and plastic gloves (Carl Roth). Seawater samples in this work were obtained from the whole water column using modified Teflon coated PVC General Oceanics (Miami, FL, USA) GoFlo bottles of 8 L in which the original drain cock was replaced by a Teflon stop cock. These bottles were deployed on a Kevlar line from the side of the ship. Immediately upon recovery of the bottles, samples were filtered in-line through 0.2 µm filter cartridges (Sartorious Sartobran filter capsule 5231307H5) by slight N_2 overpressure into acid cleaned 1 L PTFE bottles for O_2^- and into LDPE bottles for trace metal analysis (both Nalgene).

Experimental Details

Ultrapure (UP) water (resistivity > 18.2 MΩ cm^{-1}) for the total dissolved trace metal analysis was obtained in the laboratory in Kiel from a Millipore Synergy 185 system that was feed by an Elix-3 (Millipore) reverse osmosis system connected to the mains supply.

Ultrapure HNO_3 and HCl were obtained by quartz (hereafter denoted as Q-HNO_3 and Q-HCl) sub-boiling distillation from analytical grade acids (Merck) in the laboratory in Kiel. For comparison purposes a commercial source of ultrapure HCl was also used in analysis (J.T. Baker, ULTREX II). Pipettes (Finnpipette) were calibrated frequently and trace metal clean pipette tips (Rainin RT-250 and RT-1000) were used as supplied. An inoLab pH 720 (WTW) was used to determine pH values on the NBS scale.

All plasticware and bottles (low density high polyethylene (LDPE) and Polytetrafluoroethylene (PTFE)) were extensively cleaned according to the GEOTRACES trace metal clean protocols [1]. In brief this consisted of sequential cleaning in a detergent solution and then soaking in acids for a period of weeks, followed by rinsing in UP water and drying on a Class 5 laminar flow bench before double bagging in polyethylene re-lockable zipper bags (Minigrip^{TM}). All reagents and seawater samples were stored in these cleaned bottles. All the seawater used for O_2^- experiments was stored in PTFE bottles and the experiments also performed in these. Samples for dissolved trace metal analysis (filtered through 0.2 µm) were directly acidified with Q-HCl to pH<2, under a class 100-laminar flow bench. Sample processing and analysis steps were performed in laminar flow benches inside a class 100 clean room in Kiel.

Determination of Mn, Fe, Cu and Ni in seawater. Dissolved total trace metal (Copper (Cu), Iron (Fe) and Nickel (Ni)) concentrations were determined in the clean laboratory of the GEOMAR in Kiel using the graphite furnace atomic absorption (ETAAS, Perkin-Elmer Model 4100ZL) method after pre-concentration by simultaneous dithiocarbamate-freon extraction from seawater (250 - 300 g) [2-4]. Dissolved Manganese (Mn) was also analysed in the clean laboratory in Kiel by graphite furnace atomic absorption (ETAAS, Perkin-Elmer Model 4100ZL) after solvent extraction modified after[5]. The accuracy of the analytical procedures were evaluated by measurement of the SAFe intercomparison consensus samples [6, 7]. Our SAFe data is presented alongside the consensus values below. The precision for replicate analysis was between 3-5 % at the concentrations found in this study. The complete data set for the dissolved total trace metal concentrations are given in Table S3. The accuracy of the method was evaluated by measuring SAFe and GEOTRACES intercalibration samples. Our SAFe data are listed below and close to the average consensus[8]. The precision for replicate analysis was between 3 - 5% at the concentrations found in this study. The procedural (analytical) blank was 0.041 ± 0.024(σ_{bl}) nmol L^{-1} (Fe) and <1 pmol L^{-1} (Cu).

dissolved trace metal	SAFe Reference Sample	Our data (nmol L^{-1})[(a)]	Consensus values (nmol L^{-1})[(b)]
Cu	S	0.40 ± 0.03	0.52 ± 0.05
	D2	2.22 ± 0.23	2.28 ± 0.15
Fe	S	0.112 ± 0.013	0.093 ± 0.008
	D2	0.95 ± 0.28	0.933 ± 0.023
Mn	D2	0.42 ± 0.05	0.35 ± 0.06
Ni	S	1.74 ± 0.14	2.2 ± 0.09
	D2	8.44 ± 0.04	8.63 ± 0.26

(a) The errors presented with our data in this table correspond to the standard deviation as 95 % confidential interval. Our data (n = 4) was measured between January 2009 and March 2013.

(b) Note that in contrast to our data the errors presented with the consensus values in this table correspond to only 1 standard deviation (1 σ).

Calibration of the initial superoxide concentration. In the present work we routinely measured the absorbance of the standard solution of KO_2 using UV spectrophotometry with either a 1 m LWCC-2100 (100 cm) pathlength liquid waveguide cell (World Precision Instruments, Sarasota, FL, USA) and an Ocean Optics USB4000 UV-VIS spectrophotometer in combination with an Ocean Optics DT-MINI-2-GS light source. Concentrations of H_2O_2 and O_2^- were determined by determining the least squares solution to the measured absorbance, at multiple wavelengths, by using published molar extinction coefficients for H_2O_2 [9, 10] and O_2^- [11]. Mean initial concentrations in the primary KO_2 solution assessed in this way during this work (a lower strength KO_2 solution was used than previously) were 180 ± 10 µM for H_2O_2 and 18 ± 2 µM O_2^-. No DTPA or other complexing agents were added to our KO_2 primary solution. H_2O_2 in the final seawater solutions was also assessed on occasion by a chemiluminescence flow injection method described previously[12] and the results agreed well with the concentrations determined by direct spectrophotometry. For more information on specific calibration issues for O_2^- the reader is referred to our earlier work [13].

Overview of the FeLume chemiluminescence system. This system comprises a light tight box equipped with a Plexiglas spiral flow cell mounted below a photon counter (Hamamatsu HC-135-01) linked to a laptop computer via a Bluetooth connection controlled through a purpose built Labview^{TM} (National Instruments) virtual instrument. For O_2^- determination we ran the sample and the MCLA reagent directly into the flow cell using a peristaltic pump (Rainin^{TM}, operating at 16.00 rpm,) with the sample line being pulled through the flow cell as this leads to the smallest amount of dead time in the system (typically 2 – 3 s). The overall flow rate through the cell was 8.25 mL min^{-1}, comprising 5.0 mL min^{-1} from the MCLA and 3.25 mL min^{-1} from the sample. The transit time through the optical cell (300 µL) was therefore 2.18 s.

Calculation of rate data for superoxide. The raw chemiluminescence signal for the reaction between MCLA and O_2^- recorded by the computer was processed using a specially designed Labview^{TM} VI constructed for this purpose using standard kinetic fitting procedures to determine both the 1st (k_{obs}) and 2nd order (k_2) rates simultaneously. The photon counter has a base counting period of 10 ms, for the present work we used average counts of an integration time of 200 ms. Dark background counts for this detector were typically 60 – 120 counts s^{-1}. Apparent reaction rates for Mn (k_{Mn}), Cu (k_{Cu}) and Fe (k_{Fe}) with O_2^- were calculated via linear regression of k_{obs} versus the total metal added [14]. Using our experimental setup the minimum quantifiable values for k_{Mn}, k_{Cu} and k_{Fe} is estimated at 1 x 10^6 M s^{-1}.

Model Calculations for O_2^- kinetics. Numerical modelling of O_2^- reactions in seawater was performed using a fully explicit model written in C++ updated from an earlier version[15] to include Mn chemistry. Rate constants for the key reactions involved were compiled from those already published in the literature (see Table S2).

Table S1. Location of the 6 sampled GoFlo-Stations on M83/1.

Station	**Date** **dd.mm.yy**	**Time** **(UTC)**	**Latitude**	**Longitude**	**Depth** **(m)**
GOFLO1 ME831/769-1	17.10.10	23:15	17° 39.01' N	24° 15.01' W	3593.7
GOFLO2 ME831/798-1	22.10.10	06:18	12° 30.06' N	17° 37.36' W	649.9
GOFLO3 ME831/831-1	26.10.10	07:00	09° 59.99' N	16° 59.98' W	444.0
GOFLO4 ME831/861-1	30.10.10	09:48	07° 59.96' N	25° 29.98' W	4923.8
GOFLO5 ME831/881-1	03.11.10	09:13	10° 00.06' N	24° 59.99' W	5475.1
GOFLO6 ME831/912-1	08.11.10	06:46	01° 57.94' N	23° 00.06' W	4263.0

Table S2. 2nd Order Reaction Rate Constants (M^{-1} s^{-1}) for Metal species with O_2^- modified after Heller and Croot (2010) [16].

Species	HO_2	O_2^-
Cu(I)	$> 1*10^9$ (a)	$\sim 1*10^{10}$ (a)
	-	$9.4\pm0.8*10^9$ (b)
	-	$1.98\pm0.05*10^9$ (c)
Cu(II)	$1.2*10^8$ (d)	$1.1*10^{10}$ (d)
	-	$6.63 \pm 0.71*10^8$ (c)
Fe(II)	$1.2\pm0.5*10^6$ (e)	$7.2*10^8$ (f)
	$1.2\pm0.2*10^6$ (g)	$1.0\pm0.1*10^7$ (g)
Fe(III)	-	$1.8*10^8$ (g)
	$3.1*10^5$ (h)	$1.5\pm0.2*10^8$ (i)
Mn(II)		$5.4*10^7$ (j)
		$2.8*10^7$ (k)
		$1.7*10^7$ (l)
Mn(III)		$8.9*10^6$ (m)
HO_2	$8.3\pm0.7*10^5$ (n)	$9.7\pm0.6*10^7$ (n)
Cu(II)L	-	$2.9\text{-}8.1*10^8$ (o)
	-	$5\pm3*10^7$ (p)
Fe(III)L	-	$9.3\pm0.2*10^3$ (q)
	-	$2.3\pm0.1*10^5$ (r)

Notes: The reader is also referred to the compilation of Bielski et al. [11]. In describing the experimental setup used in each work we use the following abbreviations: pulse radiolysis (p.r.), flash photolysis (f.p.), γ irradiation (γ-r), optical detection of superoxide (opt) and chemical detection of superoxide or equivalent (chem.). The pKa for HO_2 is 4.60±0.15 [17]. All experiments are in the range 20-25° C.

(a)Cu^+, pH 5.3, p.r. opt. [18]. (b)Cu^+, p.r. opt. [19]. (c)Cu^+ and Cu^{++} in seawater, p.r. opt. [20]. (d)Cu^{2+} and Cu^{2+}-arginine, p.r, opt.[21]. (e)Fe^{2+}, pH 1, p.r, opt.[22]. (f)Fe^{2+} and Fe^{3+}, p.r., opt [23]. (g)Fe^{2+} species, pH 1-7, p.r, opt [24]. (h)Fe^{3+} species, pH 2.74, p.r., opt [25]. (i)$Fe(OH)^{2+}$ species, pH 1-7, p.r, opt [24]. (j) Mn^+ in sulphate, pH 7, γ-r, opt [26]. (k) Mn^+ in phosphate, pH 7, γ-r, opt[26]. (l) Mn^+ in pyrophosphate, pH 7, γ-r, opt[26]. (m)Mn^{3+} in phosphate, pH 7, γ-r, opt[26]. (n)As summarized in Bielski et al. [11]. (o)Natural seawater with Cu complexing ligands [14]. (p)Copper complexing ligands produced by *Synechococcus* [14]. (q)Fe(III) complexed with desferrioxamine B in bicarbonate buffered solution [27]. (r)Fe(III) complexed with natural organic matter in bicarbonate buffered solution [27].

Table S3: M83/1 GoFlo-Station, depth (m) and total Cu, Fe, Mn and Ni (nM) concentrations measured by ETAAS. Numbers in brackets indicate samples suspected of contamination.

Station – Depth	Cu [nM]	Fe [nM]	Mn [nM]	Ni [nM]
1 – 19 m	0.74	1.02	2.45	5.49
1 – 40 m	-	-	2.06	-
1 – 140 m	0.83	0.72	0.59	2.32
1 – 200 m	0.63	0.90	1.65	2.28
1 – 600 m	1.00	1.33	0.62	6.07
2 – 46 m	0.85	1.23	2.7	3.02
2 - 59 m	0.91	2.17	3.36	3.05
2 – 80 m	0.69	1.45	1.26	2.56
2 – 96 m	0.83	2.54	0.88	5.37
2 – 109 m	(1.91)	1.36	3.52	(14.07)
2 - 200 m	0.78	4.48	1.08	3.87
2 – 304 m	0.82	2.26	0.55	3.99
2 – 391 m	0.86	5.21	0.91	(7.46)
3 – 20 m	0.94	0.55	3.08	3.51
3 – 40 m	0.88	0.88	1.73	2.62
3 – 80 m	1.02	0.71	0.62	2.83
3 – 100 m	0.77	1.77	0.83	3.05
3 – 200 m	0.92	1.52	0.57	3.49
3 – 300 m	0.78	1.74	0.57	4.12
3 – 400 m	0.92	2.03	0.68	5.23
4 – 20 m	0.55	0.85	2.25	2.47

4 – 40 m	0.59	0.75	2.30	1.55
4 – 60 m	0.60	0.31	1.29	1.43
4 – 80 m	0.61	0.32	1.17	4.21
4 – 100 m	0.53	0.69	1.02	2.39
4 – 200 m	0.65	1.36	0.42	2.79
4 – 300 m	0.59	1.07	0.42	3.46
4 – 400 m	0.82	1.30	0.46	(9.95)
5 – 20 m	0.68	1.25	2.54	2.27
5 – 40 m	0.67	0.46	1.92	2.01
5 – 60 m	0.51	0.22	1.50	1.26
5 – 80 m	0.65	0.30	1.17	5.42
5 – 100 m	0.71	0.89	0.72	3.61
5 – 200 m	0.69	1.40	032	3.43
5 – 300 m	0.71	1.08	0.38	3.14
5 – 400 m	0.76	1.40	0.46	5.27
6 – 20 m	0.51	0.42	2.37	1.40
6 – 40 m	0.59	0.57	2.09	1.59
6 – 60 m	0.61	0.20	1.87	1.65
6 – 80 m	0.52	0.15	1.28	2.64
6 – 100 m	0.69	0.33	0.83	3.35
6 – 200 m	0.70	0.84	0.40	3.39
6 – 300 m	0.66	0.86	0.32	3.15
6 – 400 m	0.81	0.96	0.33	5.49

Notes: The accuracy of the method was evaluated by measuring SAFe and GEOTRACES intercalibration samples. Our SAFe data are listed above along with the current consensus values [8].

Table S4: Compilation of specific metal decay rates of O_2^- in Eastern Tropical north Atlantic seawater measured during M83/1 and the values (in brackets) calculated by least squares multiple regression analysis tool in Excel™.

Station – Depth	log k_{Cu}	$k_{int}Cu$	log k_{Fe}	$k_{int}Fe$	log k_{Mn}	$k_{int}Mn$	k_{SW}	k_{DTPA}
1 – 19 m	7.44 ± 0.12 (7.25 ± 0.25)	0.034 ± 0.077	7.14 ± 0.08 (6.93 ± 0.44)	0.004 ±0.003	7.18 ± 0.08 (6.88 ± 0.35)	0.036 ± 0.004	0.038	0.010 (0.006 ± 0.017)
1 – 40 m	7.30 ± 0.05 (6.97 ± 0.48)	0.043 ± 0.002	6.35 ± 0.09 (-)	0.043 ± 0.001	7.40 ± 0.04 (7.15 ± 0.21)	0.041 ± 0.003	0.043	0.030 (0.024 ± 0.018)
1 – 140 m	7.33 ± 0.15 (7.17 ± 0.24)	0.022 ± 0.008	7.00 ± 0.17 (7.73 ± 0.6)	0.023 ± 0.005	6.13 ± 0.03 (7.03 ± 0.3)	0.024 ± 0.001	0.025	0.014 (0.008 ± 0.013)
1 – 200 m	7.36 ± 0.01 (7.36 ± 0.15)	0.040 ± 0.001	6.88 ± 0.52 (6.59 ± 0.73)	0.035 ± 0.010	7.06 ± 0.11 (7.02 ± 0.27)	0.038 ± 0.004	0.039	0.020 (0.017 ± 0.012)
1 – 600 m	7.42 ± 0.11 (7.25 ± 0.3)	0.031 ± 0.007	7.37 ± 0.20 (7.14 ± 0.32)	0.028 ± 0.013	- (-)	0.035 ± 0.002	0.034	0.014 (0.008 ± 0.020)
2 – 46 m	7.73 ± 0.13	0.064 ± 0.027	6.43 ± 0.14	0.077 ± 0.002	7.29 ± 0.17	0.070 ± 0.014	0.076	0.031

	(7.79 ± 0.23)		(-)		(6.84 ± 0.88)			(0.021 ± 0.053)
2 - 59 m	7.30 ± 0.17 (7.56 ± 0.43)	0.078 ± 0.013	< 6.0 (-)	0.062 ± 0.054	< 6.0 (6.82 ± 1.24)	0.090 ± 0.000	0.086	0.036 (0.033 ± 0.061)
2 – 80 m	6.55 ± 0.12 (6.72± 0.11)	0.040 ± 0.002	< 6.0 (5.68 ± 0.96)	0.040 ± 0.000	6.70 ± 0.05 (6.85 ± 0.06)	0.039 ± 0.001	0.040	0.024 (0.023 ± 0.002)
2 – 96 m	6.38 ± 0.04 (6.49 ± 0.17)	0.036 ± 0.000	6.31 ± 0.04 (6.40 ± 0.14)	0.036 ± 0.000	6.58 ± 0.05 (6.81 ± 0.06)	0.035 ± 0.001	0.036	0.019 (0.019 ± 0.002)
2 – 109 m	- (6.65 ± 1.74)	0.031 ± 0.020	- (-)	0.021±0.0019	6.35 ± 0.28 (6.65 ± 2.55)	0.021 ± 0.003	0.022	0.015 (0.015 ± 0.025)
2 - 200 m	6.38 ± 0.03 (-)	0.035 ± 0.000	- (-)	0.037 ± 0.005	7.24 ± 0.02 (7.34 ± 0.08)	0.034 ± 0.001	0.034	0.027 (0.025 ± 0.009)
2 – 304 m	6.94 ± 0.16 (6.95 ± 0.42)	0.023 ± 0.005	6.83 ± 0.09	0.019 ± 0.000	6.81 ± 0.14 (6.47 ± 0.80)	0.020 ± 0.004	0.021	0.016 (0.012 ± 0.014)
2 – 391 m	6.56 ± 0.15 (6.73 ± 0.32)	0.026 ± 0.002	- (-)	0.029 ± 0.005	6.67 ± 0.00 (6.84 ± 0.37)	0.027 ± 0.000	0.027	0.022 (0.021 ± 0.006)

3 – 20 m	7.70 ± 0.14 (7.97 ± 0.21)	0.058 ± 0.017	7.82 ± 0.19 (7.68 ± 0.39)	0.080 ± 0.034	7.30 ± 0.01 (-)	0.065 ± 0.001	0.065	0.045 (0.030 ± 0.077
3 – 40 m	6.24 ± 1.27 (6.5 ± 0.52)	0.059 ± 0.005	6.67 ± 0.16 (6.84 ± 0.22)	0.060 ± 0.002	7.08 ± 0.08 (7.14 ± 0.21)	0.060 ± 0.003	0.061	0.089 (0.024 ± 0.007)
3 – 80 m	7.13 ± 0.16 (6.98 ± 0.20)	0.027 ± 0.004	- (-)	0.030 ± 0.002	7.30 ± 0.01 (7.27 ± 0.09)	0.029 ± 0.000	0.029	0.027 (0.013 ± 0.007)
3 – 100 m	6.42 ± 2.79 (6.78 ± 0.91)	0.039 ± 0.017	- (-)	0.031 ± 0.001	7.42 ± 0.02 (7.37 ± 0.19)	0.031 ± 0.001	0.036	0.030 (0.017 ± 0.021)
3 – 200 m	- (-)	0.031 ± 0.002	- (-)	0.030 ± 0.004	7.54 ± 0.15 (7.51 ± 0.13)	0.025 ± 0.016	0.044	0.016 (0.014 ± 0.019)
3 – 300 m	6.86 ± 0.29 (6.91 ± 0.18)	0.034 ± 0.005	- (-)	0.035 ± 0.004	7.40 ± 0.01 (7.45 ± 0.04)	0.036 ± 0.000	0.037	0.035 (0.016 ± 0.006)
3 – 400 m	6.51 ± 4.22 (7.05 ± 0.9)	0.044 ± 0.032	- (-)	0.028 ± 0.005	7.35 ± 0.03 (7.31 ± 0.42)	0.031 ± 0.002	0.030	0.016 (0.019 ± 0.039)
4 – 20 m	6.85 ± 1.35	0.045 ± 0.001	7.22 ± 0.11	0.048 ± 0.005	7.57±0.04	0.048 ± 0.004	0.046	0.017

	(-)		(6.50 ± 2.16)		(7.38 ± 0.19)			(0.011 ± 0.030)
4 – 40 m	6.14 ± 0.95 (-)	0.045 ± 0.003	6.98 ± 0.45 (6.97 ± 1.01)	0.049 ± 0.011	6.71 ± 2.12 (7.07 ± 0.52)	0.058 ± 0.032	0.044	0.014 (0.018 ± 0.040)
4 – 60 m	< 6.0 (-)	0.034 ± 0.003	6.88 ± 0.04 (6.58 ± 0.71)	0.033 ± 0.001	7.22 ± 0.08 (7.07 ± 0.17)	0.031 ± 0.004	0.033	0.028 (0.023 ± 0.0103)
4 – 80 m	- (6.34 ± 1.44)	0.046 ± 0.003	- (-)	0.044 ± 0.008	6.72 ± 0.08 (7.05 ± 0.2)	0.047 ± 0.001	0.048	0.021 (0.024 ± 0.011)
4 – 100 m	7.31 ± 0.37 (7.13 ± 0.32)	0.028 ± 0.018	6.83 ± 0.49 (6.51 ± 1.16)	0.032 ± 0.009	7.20 ± 0.04 (7.15 ± 0.21)	0.035 ± 0.002	0.036	0.018 (0.012 ± 0.015)
4 – 200 m	6.91 ± 0.18 (6.44 ± 0.72)	0.023 ± 0.000	- (-)	0.022 ± 0.001	7.02 ± 0.01 (7.06 ± 0.15)	0.021 ± 0.000	0.021	0.012 (0.014 ± 0.073)
4 – 300 m	6.37 ± 0.16 (6.19 ± 0.38)	0.015 ± 0.001	< 6.0 (5.87 ± 0.63)	0.016 ± 0.001	6.90 ± 0.07 (6.9 ± 0.06)	0.016 ± 0.002	0.015	0.011 (0.011 ± 0.0 21)
4 – 400 m	6.56 ± 0.06 (6.37 ± 0.49)	0.016 ± 0.000	6.34 ± 0.06 (5.99 ± 0.95)	0.017 ± 0.000	7.04 ± 0.08 (6.99 ± 0.1)	0.017 ± 0.000	0.017	0.011 (0.010 ± 0.004)

5 – 20 m	No data	No data	No data	No data	No data	No data	No data	No data
5 – 40 m	No data	No data	No data	No data	No data	No data	No data	No data
5 – 60 m	6.54 ± 0.24 (6.69 ± 0.27)	0.032 ± 0.002	- (-)	0.032 ± 0.001	6.92 ± 0.09 (6.90 ± 0.12)	0.031 ± 0.002	0.031	0.017 (0.019 ± 0.005)
5 – 80 m	No data	No data	No data	No data	No data	No data	No data	No data
5 – 100 m	6.45 ± 0.00 (6.6 ± 0.19)	0.020 ± 0.000	- (5.82 ± 0.99)	0.020 ± 0.001	6.96 ± 0.04 (7.01 ± 0.66)	0.021 ± 0.001	0.020	0.010 (0.011 ± 0.003)
5 – 200 m	6.50 ± 0.20 (-)	0.014 ± 0.002	- (7.47 ± 0.45)	0.085 ± 0.157	7.09 ± 0.02 (-)	0.015 ± 0.001	0.015	0.007 (0.019 ± 0.007)
5 – 300 m	6.09 ± 0.36 (6.06 ± 0.76)	0.012 ± 0.001	Below detection (6.23 ± 0.42)	0.014 ± 0.002	6.99 ± 0.07 (7.02 ± 0.07)	0.014 ± 0.002	0.013	0.006 (0.007 ± 0.000)
5 – 400 m	No data	No data	No data	No data	No data	No data	No data	No data
6 – 20 m	7.16 ± 0.00 (7.11 ± 0.17)	0.048 ± 0.000	6.86 ± 0.02 (6.77 ± 0.33)	0.048 ± 0.000	7.35 ± 0.08 (7.29 ± 0.07)	0.064 ± 0.005	0.048	0.050 (0.007 ± 0.008)

6 – 40 m	< 6.0 (6.96 ± 0.37)	0.053 ± 0.001	6.25± 0.96 (6.89 ± 0.40)	0.052 ± 0.005	7.17 ± 0.09 (7.31 ± 0.12)	0.052 ± 0.004	0.054	0.044 (0.014 ± 0.012)
6 – 60 m	6.79 ± 0.94 (7.16 ± 0.69)	0.057 ± 0.014	- (-)	0.065 ± 0.005	- (7.16 ± 0.45)	0.070 ± 0.015	0.063	0.051 (0.020 ± 0.035)
6 – 80 m	- (7.02 ± 0.59)	0.053 ± 0.020	< 6.0 (6.85 ± 0.86)	0.049 ± 0.010	6.91 ± 0.06 (7.12 ± 0.37)	0.045 ± 0.002	0.044	0.040 (0.023 ± 0.021)
6 – 100 m	6.97 ± 0.22 (-)	0.009 ± 0.005	6.33 ± 0.14 (-)	0.010 ± 0.001	- (7.66 ± 0.51)	(-)	0.044	0.045 (0.026 ± 0.095)
6 – 200 m	6.38 ± 0.04 (6.41 ± 0.36)	0.011 ± 0.000	- (-)	0.011 ± 0.001	7.08 ± 0.07 (7.10 ± 0.07)	0.012 ± 0.003	0.011	0.011 (0.007 ± 0.003)
6 – 300 m	No data	(-)	6.20 ± 0.04 (-)	0.009 ± 0.010	7.24 ± 0.31 (-)	0.016 ± 0.060	0.009	- (-)
6 – 400 m	6.85 ± 0.34 (6.51 ± 0.77)	0.065 ± 0.006	< 6.0 (-)	0.010 ± 0.002	7.17 ± 0.10 (7.10 ± 0.16)	0.011 ± 0.005	0.009	0.011 (0.006 ± 0.009)

Notes: 95% CI listed for lower data.

Table S5: Compilation of ranges of specific metal reactions of superoxide in seawater during M83/1 and from other studies.

Study	Cruise	Station	Depth	Cu [nM]	Fe [nM]	Mn [nM]	log k_{Cu}	log k_{Fe}	log k_{Mn}	k_{SW}	k_{DTPA}
This study	RV Meteor M83/1 ETNA	GoFlo 1 (CVOO)	19-600	0.63-1.00	0.72-1.32	0.59-2.06	7.30-7.44	6.35-7.37	6.13-7.40	0.025-0.043	0.010-0.030
		GoFlo 2	46-391	0.7-0.90	1.23-5.21		6.38-6.94	< 6-6.83	< 6-7.24	0.021-0.086	0.016-0.36
		GoFlo 3	20-400	0.78-1.02	0.55-2.02	0.57-3.08	6.24-7.70	6.67-7.82	7.08-7.54	0.029-0.065	0.016-0.089
		GoFlo 4	20-400	0.55-0.82	0.31-1.36	0.42-2.30	< 6-7.31	< 6-7.22	6.71-7.57	0.015-0.048	0.011-0.028
		GoFlo 5	20-400	0.51-0.76	0.22-1.40	0.31-2.54	6.09-6.54	< 6-7.47	6.92-7.09	0.013-0.031	0.006-0.017
		GoFlo 6	20-400	0.51-0.80	0.15-0.97		< 6.-7.16	< 6-6.86	6.91-7.35	0.009-0.063	0.011-0.051
[28]Hansard et al., 2011	GoA1-4 Gulf of Alaska					Added Mn: 3-24			6.78-7.00		
[16]Heller and Croot, 2010a	RV Polar-stern (ANT24/3) Antarctica	230-6	25-1000	1.4-1.89	0.346-1.78		7.27-7.85	< 6-7.64		0.014-0.041	2.00×10^5-9.36×10^4

		236-5	25-2800	1.07-1.95	0.109-1.91		< 6-7.79	< 6-7.43		0.008-0.037	$1.77x10^{5}$-$7.21x10^{4}$
		249-3	25-1000	0.85-2.27	0.22-0.666		6.4-7.9	< 6-7.79		0.009-0.021	$1.17x10^{5}$-$4.46x10^{4}$
[29]Heller and Croot, 2010b	RV Islandia ETNA	10 (CVOO)	10	0.78	0.6		7.5	7.19		0.023	0.013
[30]Heller and Croot, 2011	RV Islandia ETNA	8	5	0.68	0.81		7.4	6.28		0.036	0.013

[14]Voelker et al., 2000							*log $k_{CuL1:}$ < 8.00 log k_{CuL2}: 8.46-8.91				

Table S6: Normalized estimated % for each reaction pathway by multiple linear regression and used in the pie charts.

Station - Depth	%DTPA	%Cu	%Fe	%Mn
1 – 19 m	12 ± 38	29 ± 17	19 ± 20	39 ± 31
1 – 40 m	39 ± 29	13 ± 15	0	47 ± 22
1 – 140 m	29 ± 47	43 ± 23	14 ± 19	14 ± 9
1 – 200 m	44 ± 31	36 ± 12	9 ± 15	11 ± 7
1 – 600 m	18 ± 50	40 ± 28	42 ± 31	0
2 – 46 m	20 ± 51	50 ± 26	0	29 ± 59
2 - 59 m	36 ± 66	36 ± 36	0	28 ± 80
2 – 80 m	60 ± 6	9 ± 2	2 ± 0	29 ± 4
2 – 96 m	55 ± 6	8 ± 3	11 ± 0	26 ± 4
2 – 109 m	44 ± 76	25 ± 101	0	31 ± 183
2 - 200 m	No data	No data	No data	No data
2 – 304 m	50 ± 59	29 ± 28	10 ± 0	11 ± 25
2 – 391 m	60 ± 28	13 ± 10	0	27 ± 23
3 – 20 m	78 ± 33	0	0	22 ± 0
3 – 40 m	42 ± 12	5 ± 6	11 ± 10	42 ± 8
3 – 80 m	44 ± 18	19 ± 8	0	37 ± 6
3 – 100 m	41 ± 52	11 ± 24	0	48 ± 21
3 – 200 m	43 ± 57	0	0	57 ± 17
3 – 300 m	41 ± 15	17 ± 7	0	43 ± 4
3 – 400 m	44 ± 94	24 ± 50	0	32 ±31
4 – 20 m	14 ± 29	0	6 ± 18	80 ± 23

4 – 40 m	No data	No data	No data	No data
4 – 60 m	58 ± 26	0	3 ± 5	39 ± 15
4 – 80 m	63 ± 29	3 ± 11	0	34 ± 16
4 – 100 m	34 ± 43	20 ± 15	6 ± 17	40 ± 21
4 – 200 m	69 ± 35	9 ± 14	0	23 ± 8
4 – 300 m	69 ± 13	5 ± 5	5 ± 7	21 ± 3
4 – 400 m	59 ± 11	11 ± 5	8 ± 7	22 ± 3
5 – 20 m	No data	No data	No data	No data
5 – 40 m	No data	No data	No data	No data
5 – 60 m	62 ± 15	8 ± 5	0	30 ± 8
5 – 80 m	No data	No data	No data	No data
5 – 100 m	57 ± 15	15 ± 7	3 ± 0	25 ± 4
5 – 200 m	32 ± 109	0	68 ± 75	0
5 – 300 m	55 ± 25	6 ± 11	14 ± 19	24 ± 4
5 – 400 m	No data	No data	No data	No data
6 – 20 m	15 ± 16	13 ± 5	5 ± 4	67 ± 11
6 – 40 m	31 ± 28	12 ± 10	10 ± 9	46 ± 13
6 – 60 m	39 ± 71	17 ± 27	0	43 ± 45
6 – 80 m	59 ± 52	14 ± 19	3 ± 5	25 ± 21
6 – 100 m	59 ± 211	0	0	41 ± 49
6 – 200 m	59 ± 27	16 ± 13	0	25 ± 4
6 – 300 m	No data	No data	No data	No data
6 – 400 m	48 ± 90	22 ± 48	0	30 ± 13

Notes: 95% CI is listed for all the calculated data.

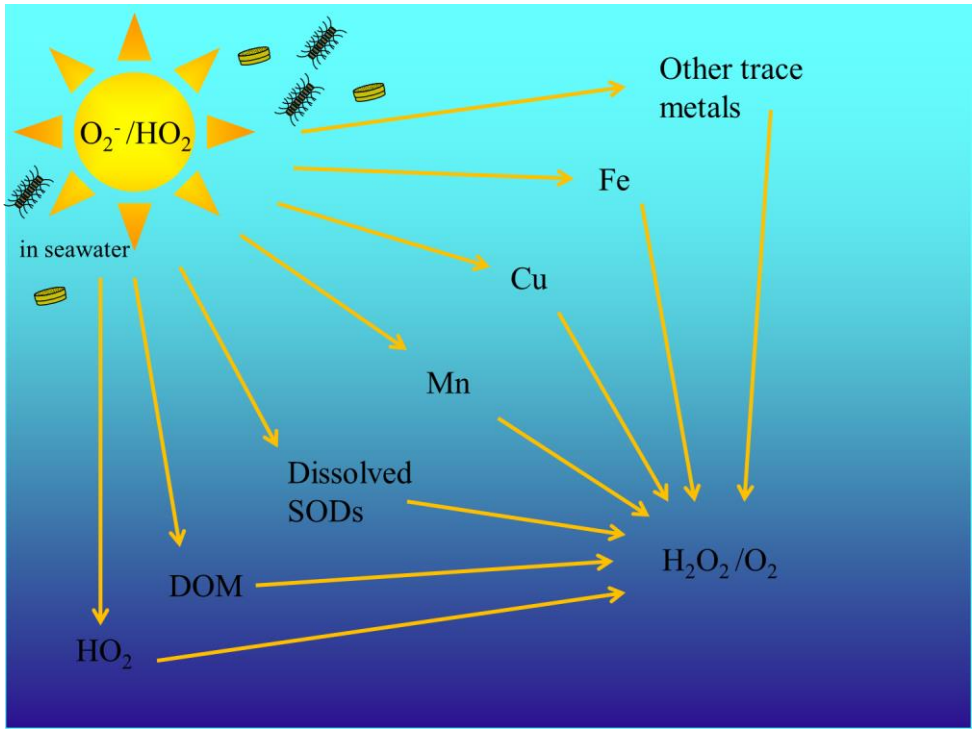

Figure S1. Schematic of the different decay pathways for O_2^- decay in the ocean. O_2^- is biologically and photo produced.

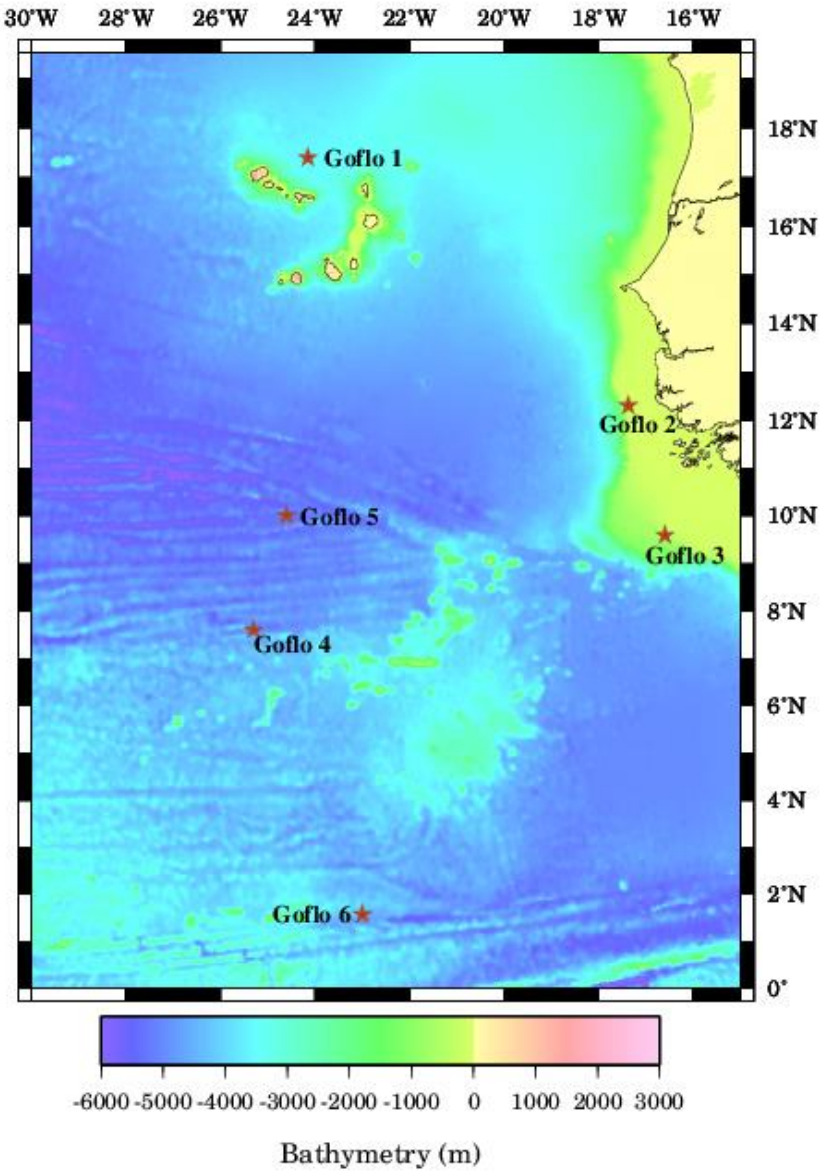

Figure S2: Map showing the location of the 6 GoFlo sampling stations in this work (M83/1).

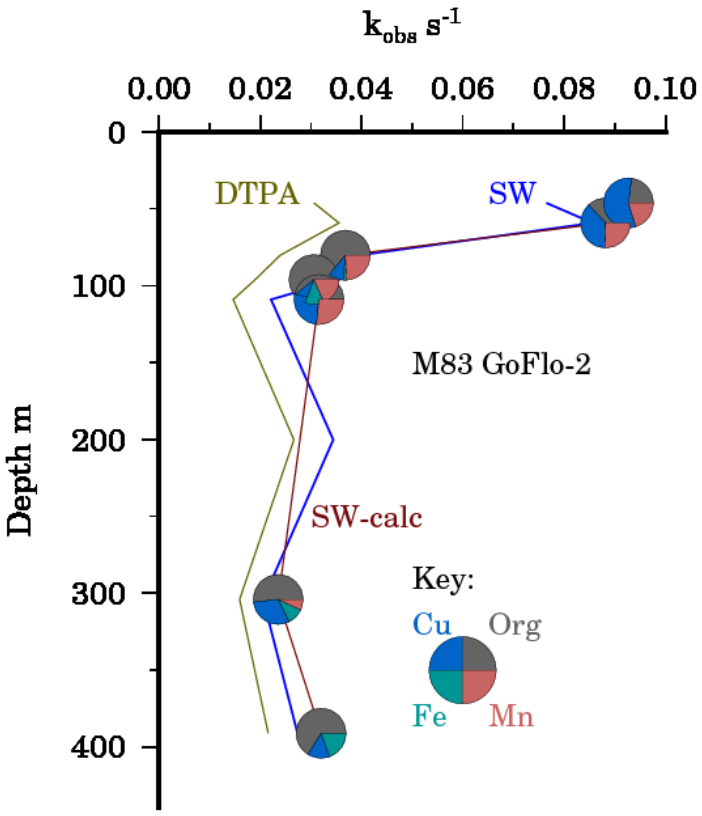

Figure S3: In this depth profile of observed loss rate of O_2^-, k_{obs}, at the GOFLO-Station 2 (on the shelf). The reaction with organic matter, k_{org}, is assumed to be equal to the measured reaction when DTPA is added, k_{DTPA} (beige line). k_{SW} is the reaction measured in unamended seawater (blue line). $k_{SW\text{-}calc}$ is the calculated reaction with seawater (red line). With the help of the pie-charts the contribution from Organic matter, Cu, Fe and Mn on $k_{sw\text{-}cal}$ is shown as explained for Figure 2 in the manuscript.

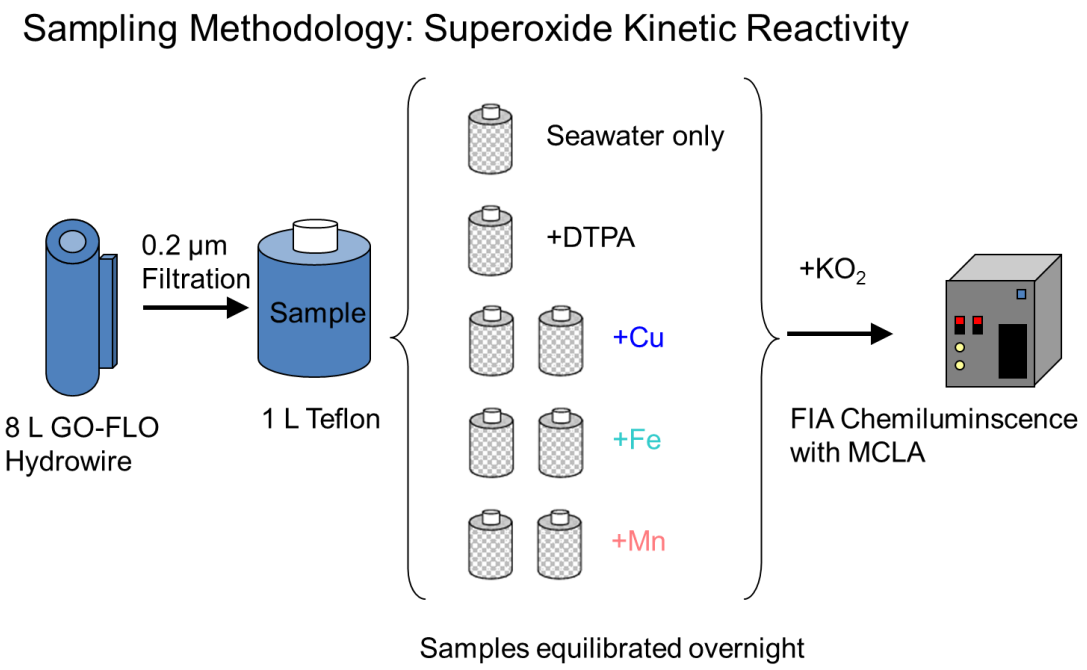

Figure S4: Experimental design and description of the sampling protocol employed in this work which was further developed according to our previous work [16].

References:

1. Cutter, G. A.; Andersson, P.; Codispoti, L.; Croot, P. L.; Francois, R.; Lohan, M.; Obata, H.; Rutgers van der Loeff, M. Sampling and Sample-handling Protocols for GEOTRACES Cruises. http://www.geotraces.org/libraries/documents/Intercalibration/Cookbook.pdf
2. Bruland, K. W.; Franks, R. P.; Knauer, G. A.; Martin, J. H., Sampling and Analytical Methods for the Determination of Copper, Cadmium, Zinc, and Nickel at the Nanogram Per Liter Level in Sea-Water. *Anal Chim Acta* **1979,** *105*, (1), 233-245.
3. Danielsson, L.-G.; Magnusson, B.; Westerlund, S., An improved metal extraction procedure for the determination of trace metals in sea water by atomic absorption spectrometry with electrothermal atomization. *Anal Chim Acta* **1978,** *98*, (1), 47-57.
4. Grasshoff, K.; Kremling, K.; Ehrhardt, M., *Methods of seawater analysis*. Verlag Chemie: Weinheim, 1983.
5. Klinkhammer, G. P., Determination of manganese in sea water by flameless atomic absorption spectrometry after preconcentration with 8-hydroxyquinoline in chloroform. *Anal. Chem.* **1980,** *52*, (1), 117-120.
6. Johnson, K. S.; Boyle, E.; Bruland, K.; Coale, K.; Measures, C.; Moffett, J.; Aguilar-islas, A.; Barbeau, K.; Berquist, B.; Bowie, A.; Buck, K.; Cai, Y.; Chase, Z.; Cullen, J.; Doi, T.; Elrod, V.; Fitzwater, S.; Gordon, M.; King, A.; Laan, P.; Laglera-Baquer, L.; Landing, W.; Lohan, M.; Mendez, J.; Milne, A.; Obata, H.; Ossiander, L.; Plant, J.; Sarthou, G.; Sedwick, P.; Smith, G. J.; Sohst, B.; Tanner, S.; Berg, S. v. d.; Wu, J., Developing Standards for Dissolved Iron in Seawater. *EOS, Trans. Am. Geophys. Union* **2007,** *88*, (11), 131-132.
7. Johnson, K. S.; Boyle, E.; Bruland, K.; Coale, K.; Measures, C.; Moffett, J.; Aguilar-islas, A.; Barbeau, K.; Berquist, B.; Bowie, A.; Buck, K.; Cai, Y.; Chase, Z.; Cullen, J.; Doi, T.; Elrod, V.; Fitzwater, S.; Gordon, M.; King, A.; Laan, P.; Laglera-Baquer, L.; Landing, W.; Lohan, M.; Mendez, J.; Milne, A.; Obata, H.; Ossiander, L.; Plant, J.; Sarthou, G.; Sedwick, P.; Smith, G. J.; Sohst, B.; Tanner, S.; Berg, S. v. d.; Wu, J., Developing Standards for Dissolved Iron in Seawater. *EOS, Transactions of the American Geophysical Union* **2007,** *88*, (11), 131-132.
8. Bruland, K. W. Consensus Values for the GEOTRACES 2008 and SAFe Reference Samples. http://es.ucsc.edu/~kbruland/GeotracesSaFe/kwbGeotracesSaFe.html
9. Baxendale, J. H.; Wilson, J. A., The photolysis of hydrogen peroxide at high light intensities. *Trans. Faraday Soc.* **1957,** *53*, 344-356.
10. Taylor, R. C.; Cross, P. C., Light Absorption of Aqueous Hydrogen Peroxide Solutions in the Near Ultraviolet Region. *J. Am. Chem. Soc.* **1949,** *71*, (6), 2266-2268.
11. Bielski, B. H. J.; Cabelli, D. E.; Arudi, R. L.; Ross, A. B., Reactivity Of HO_2/O_2^- Radicals In Aqueous-Solution. *J. Phys. Chem. Ref. Data* **1985,** *14*, (4), 1041-1100.
12. Croot, P. L.; Streu, P.; Peeken, I.; Lochte, K.; Baker, A. R., Influence of the ITCZ on H_2O_2 in near surface waters in the equatorial Atlantic Ocean. *Geophys. Res. Lett.* **2004,** *31*, L23S04, doi:10.1029/2004GL020154.
13. Heller, M. I.; Croot, P. L., Application of a Superoxide (O_2^-) thermal source (SOTS-1) for the determination and calibration of O_2^- fluxes in seawater. *Anal Chim Acta* **2010,** *667*, 1-13.
14. Voelker, B. M.; Sedlak, D. L.; Zafiriou, O. C., Chemistry of Superoxide Radical in Seawater: Reactions with Organic Cu Complexes. *Environ. Sci. Tech.* **2000,** *34*, 1036-1042.
15. Croot, P. L.; Laan, P.; Nishioka, J.; Strass, V.; Cisewski, B.; Boye, M.; Timmermans, K.; Bellerby, R.; Goldson, L.; de Baar, H. J. W., Spatial and Temporal distribution of Fe(II) and H_2O_2 during EISENEX, an open ocean mesoscale iron enrichment. *Mar. Chem.* **2005,** *95*, 65-88.

16. Heller, M. I.; Croot, P. L., Superoxide decay kinetics in the southern ocean. *Environ. Sci. Tech.* **2010,** *44*, (1), 191-6.
17. Zafiriou, O. C., Chemistry of superoxide ion (O_2^-) in seawater. I. pK_{asw}^* (HOO) and uncatalysed dismutation kinetics studied by pulse radiolysis. *Mar. Chem.* **1990,** *30*, 31-43.
18. Rabani, J.; Klug-Roth, D.; Lilie, J., Pulse radiolytic investigations of the catalyzed disproportionation of peroxy radicals. Aqueous cupric ions. *J. Phys. Chem.* **1973,** *77*, (9), 1169-1175.
19. Piechowski von, M.; Nauser, T.; Hoigné, J.; Bühler, R., O_2^- decay catalyzed by Cu^{2+} and Cu^+ ions in aqueous solutions: a pulse radiolysis study for atmospheric chemistry. *Ber. Bunsenges. Phys. Chem.* **1993,** *6*, 762-771.
20. Zafiriou, O. C.; Voelker, B. M.; Sedlak, D. L., Chemistry of the superoxide radical (O_2^-) in seawater: Reactions with inorganic copper complexes. *J. Phys. Chem. A* **1998,** *102*, (28), 5693-5700.
21. Cabelli, D. E.; Bielski, B. H. J.; Holcman, J., Interaction between Copper(II)-Arginine Complexes and HO_2/O_2^- Radicals, a Pulse Radiolysis Study. *J. Am. Chem. Soc.* **1987,** *109*, 3665-3669.
22. Jayson, G. G.; Parsons, B. J.; Swallow, A. J., Oxidation Of Ferrous Ions By Perhydroxyl Radicals. *J. Chem. Soc. - Faraday Trans. I* **1973,** *69*, (1), 236-242.
23. Matthews, R. W., The radiation chemistry of aqueous ferrous sulfate solutions at natural pH. *Aust. J. Chem.* **1983,** *36*, 1305-1317.
24. Rush, J. D.; Bielski, B. H. J., Pulse Radiolytic Studies of HO_2/O_2^- with Fe(II)/Fe(III) Ions. The reactivity of HO_2/O_2^- with Ferric Ions and Its Implication on the Occurrence of the Haber-Weiss Reaction. *J. Phys. Chem.* **1985,** *89*, 5062-5066.
25. Sehested, K.; Bjergbakke, E.; Rasmussen, O. L.; Fricke, H., Reactions of H_2O_3 in the Pulse γ-Irradiated Fe(II)-O_2 System. *J. Chem. Phys.* **1969,** *51*, (8), 3159-3166.
26. Barnese, K.; Gralla, E. B.; Cabelli, D. E.; Selverstone Valentine, J., Manganous Phosphate Acts as a Superoxide Dismutase. *J. Am. Chem. Soc.* **2008,** *130*, (14), 4604-4606.
27. Rose, A. L.; Waite, T. D., Reduction of organically complexed ferric iron by superoxide in a simulated natural water. *Environ. Sci. Tech.* **2005,** *39*, (8), 2645-2650.
28. Hansard, S. P.; Easter, H. D.; Voelker, B. M., Rapid reaction of nanomolar Mn(II) with superoxide radical in seawater and simulated freshwater. *Environ. Sci. Tech.* **2011,** *45*, (7), 2811-7.
29. Heller, M. I.; Croot, P. L., Kinetics of superoxide reactions with dissolved organic matter in tropical Atlantic surface waters near Cape Verde (TENATSO). *J. Geophys. Res.* **2010,** *115*, (C12), C12038.
30. Heller, M. I.; Croot, P. L., Superoxide decay as a probe for speciation changes during dust dissolution in Tropical Atlantic surface waters near Cape Verde. *Mar. Chem.* **2011,** *126*, (1-4), 37-55.